Shapiro-like resonance in ultracold molecule production via an oscillating magnetic field

Bin Liu,[1,2] Li-Bin Fu,[1,3] and Jie Liu[1,3,*]

[1]*Institute of Applied Physics and Computational Mathematics, Beijing 100088, People's Republic of China*
[2]*Graduate School, China Academy of Engineering Physics, Beijing 100088, People's Republic of China*
[3]*Center for Applied Physics and Technology, Peking University, Beijing 100084, People's Republic of China*

(Received 15 May 2009; published 4 January 2010)

We study the process of the production of ultracold molecules from ultracold atoms using a sinusoidally oscillating magnetic-field modulation. Our study is based on a two-mode mean-field treatment of the problem. When the magnetic field is resonant roughly with the molecular binding energy, Shapiro-like resonances are observed. Their resonance profiles are well fitted by the Lorentzian functions. The linewidths depend on both the amplitude and the duration of the applied modulations and are found to be dramatically broadened by the thermal dephasing effect. The resonance centers shift due to both the many-body effect and the finite temperature effect. Our theory is consistent with a recent experiment [S. T. Thompson, E. Hodby, and C. E. Wieman, Phys. Rev. Lett. **95**, 190404 (2005)]. Our model predicts a 1/3 ceiling for the molecular production yield in uncondensed ultracold atomic clouds for a long coupling time, while for condensed atoms the optimal conversion yield could be beyond the limit.

DOI: 10.1103/PhysRevA.81.013602 PACS number(s): 03.75.Nt, 34.50.−s, 36.90.+f

I. INTRODUCTION

Shapiro resonance is one of the most remarkable properties of the superconducting device, in which two weakly coupled superconductors are subject to a voltage difference that is the sum of a dc component V and a periodic signal $V_m \sin(ft)$. A continuous range of nonzero dc currents are possible if $V = \frac{\hbar}{2e}kf$, where $2e$ is the Cooper-pair charge, $\hbar$ is the reduced Planck constant, and k is an integer [1,2]. The Shapiro resonance provides a method for measuring the constant of nature $2e/\hbar$ with such precision and universality [3,4] that, since 1972, the reversed view has been adopted whereby $2e/\hbar$ is assumed to be known and the above Shapiro resonance is used to define a standard unit of voltage [2,5,6].

Essentially, the Shapiro resonance is a specific phenomenon that emerges when the frequency of the external field is commensurate with the intrinsic frequency of the system. Recently, the Shapiro resonance has received renewed interest and investigations in the Bose-Einstein condensates (BECs) [7–9]. For example, in BEC Josephson junction, the dc value of the drift current shows up as resonant spikes [7]. Under experimentally accessible conditions, well-developed half-integer Shapiro-like resonances exist [8]. The Shapiro effect also allows precise measurements in atomic BECs. The ac-driven atomic Josephson devices can be used to define a standard of chemical potential [9].

In the present paper, we investigate the Shapiro resonance effects in ultracold molecule production. The conversion of ultracold atoms to ultracold molecules by time-varying magnetic fields in the vicinity of a Feshbach resonance is currently a topic of much experimental and theoretical interest. This particular conversion process lends itself well to the formation of molecular Bose-Einstein condensates [10–13] and atom-molecule superpositions [14]. These Feshbach molecules and their creation process are also important for understanding ultracold fermionic systems in the BCS-BEC crossover regime, because they are closely related to the pairing mechanism in a fermionic superfluid that occurs near a Feshbach resonance [15–18]. We study the process of production of ultracold molecules from ultracold atoms using a sinusoidally oscillating magnetic-field modulation. The advantage of this method is that it greatly reduces the heating the cloud experiences in the conversion process, because the conversion occurs far from the center of the Feshbach resonance. In recent experiments, this technique has been applied and has produced molecules from atoms more efficiently [19] and measured the binding energy of the Feshbach molecule precisely.

However, the underlying mechanism is not fully understood, and the important feature of the experimental data has not been explained yet. The complexity arises from the many-body problem and time-dependent field involved. By weighting the two-body transition probability density (primarily determined by the detuning from the resonant continuum energy) over a Maxwell distribution, a two-channel two-body model has been used to explain the experimental observations, and it provides a qualitative explanation [20]. However, the Maxwell distribution gives rise to an asymmetric distribution over the modulation frequency, prominently departing from the observed Lorentzian-like resonance profiles of symmetric property. Moreover, the above approach cannot lead to the observed saturation of the conversion efficiency. In the present paper, we exploit a many-body two-channel model to investigate thoroughly the mechanism underlying the Shapiro resonance phenomenon in the atom-molecule conversion. By quantitatively including the thermal dephasing effect in the noncondensed atom clouds, our model has accounted for most experimental observations. Our model calculation has reproduced the Lorentzian resonance line shape and explained the observed maximum conversion efficiency in terms of relaxation to a mean-field fixed point. We discuss the applicability of our model to condensed and uncondensed populations.

*liu_jie@iapcm.ac.cn

The plan of this paper is as follows. In Sec. II, we present our model and thoroughly analyze the Shapiro resonance. In Sec. III, we apply our theory to explain the recent experiment. Section IV is our conclusion.

II. SHAPIRO-LIKE RESONANCE IN ATOM-MOLECULE CONVERSION FROM A TWO-CHANNEL PERSPECTIVE

A. Model

Ignoring the two- and three-body atomic decay and collisional molecular decay, we exploit the following two-channel microscopic model to describe the dynamics of converting atoms to molecules in the bosonic system

$$\hat{H} = (\epsilon_a - \mu)\,\hat{a}^\dagger\hat{a} + [\epsilon_b + \nu(t) - 2\mu]\,\hat{b}^\dagger\hat{b} + \frac{g}{\sqrt{\mathcal{V}}}(\hat{a}^\dagger\hat{a}^\dagger\hat{b} + \hat{b}^\dagger\hat{a}\hat{a}). \tag{1}$$

Here $\hat{a}$ ($\hat{a}^+$) and $\hat{b}$ ($\hat{b}^+$) are Bose annihilation (creation) operators of atoms and molecules, respectively. The total number of particles $N = \hat{a}^\dagger\hat{a} + 2\hat{b}^\dagger\hat{b}$ is a conserved constant. The atomic and molecular kinetic energies are given by ϵ_a and ϵ_b, μ is the chemical potential, g governs the atom-molecule coupling strength, $\mathcal{V}$ denotes the quantization volume of trapped particles, and therefore $n = N/\mathcal{V}$ is the mean density of initial bosonic atoms. In Eq. (1), $\nu(t)$ represents the binding energy of diatomic molecules that depends on the external field, expressed approximately as [21]

$$\nu(t) = -\frac{\hbar^2}{m(a_{\rm eff} - r_0)^2}, \tag{2}$$

where r_0 is the effective range of the van der Waals potential, m is the mass of a bosonic atom, and $a_{\rm eff}$ denotes the effective scattering length driven by the external magnetic field,

$$a_{\rm eff} = a_{\rm bg}\left(1 - \frac{\Delta B}{B - B_0}\right), \tag{3}$$

where $a_{\rm bg}$ is the background scattering length, B_0 is the Feshbach resonance position, ΔB is the width of the resonance defined through the relation with the atom-molecule coupling term $\Delta B = mg^2/4\pi\hbar^2|a_{\rm bg}\Delta\mu|$, where $\Delta\mu$ is the difference in magnetic moment between the closed-channel and open-channel states. We focus on the situation in which the selected external field $B_{\rm ex}$ is modulated sinusoidally with small amplitude $B_{\rm mod}$ and large frequency ω near a Feshbach resonance, i.e.,

$$B(t) = B_{\rm ex} + B_{\rm mod}\sin(\omega t). \tag{4}$$

Since $B_{\rm mod} \ll B_{\rm ex}$, the binding energy can be expanded into series to the first order of $B_{\rm mod}$,

$$\nu(t) = \nu_e + \nu_m\sin(\omega t), \tag{5}$$

where

$$\nu_e = -\frac{\hbar^2}{ma_{\rm bg}^2}\frac{(B_{\rm ex} - B_0)^2}{\left[\left(1 - \frac{r_0}{a_{\rm bg}}\right)(B_{\rm ex} - B_0) - \Delta B\right]^2}, \tag{6}$$

and

$$\nu_m = \frac{\hbar^2}{ma_{\rm bg}^2}\frac{2(B_{\rm ex} - B_0)\Delta B B_{\rm mod}}{\left[\left(1 - \frac{r_0}{a_{\rm bg}}\right)(B_{\rm ex} - B_0) - \Delta B\right]^3}. \tag{7}$$

B. Shapiro-like resonance

We introduce the operators to investigate the dynamics of this system [22],

$$\hat{K}_x = \sqrt{2}\frac{\hat{a}^\dagger\hat{a}^\dagger\hat{b} + \hat{b}^\dagger\hat{a}\hat{a}}{N^{3/2}}, \tag{8}$$

$$\hat{K}_y = \sqrt{2}i\frac{\hat{a}^\dagger\hat{a}^\dagger\hat{b} - \hat{b}^\dagger\hat{a}\hat{a}}{N^{3/2}}, \tag{9}$$

$$\hat{K}_z = \frac{2\hat{b}^\dagger\hat{b} - \hat{a}^\dagger\hat{a}}{N}, \tag{10}$$

with the commutators

$$[\hat{K}_z, \hat{K}_x] = \frac{4i}{N}\hat{K}_y, \tag{11}$$

$$[\hat{K}_z, \hat{K}_y] = -\frac{4i}{N}\hat{K}_x, \tag{12}$$

$$[\hat{K}_x, \hat{K}_y] = \frac{i}{N}(1 - \hat{K}_z)(1 + 3\hat{K}_z) + \frac{4i}{N^2}, \tag{13}$$

where $\hat{K}_x$, $\hat{K}_y$ denote the coherence terms, and $\hat{K}_z$ is the population imbalance. Then the Hamiltonian can be written as

$$H = \frac{N}{4}\{[\nu_0 + \nu_m\sin(\omega t)]\hat{K}_z + \sqrt{2}\eta\hat{K}_x\}, \tag{14}$$

where $\nu_0 = \nu_e + \epsilon_b - 2\epsilon_a$ is the energy difference between atoms and molecules, and parameter $\eta = 2g\sqrt{n}$ denotes the coupling strength. Then the Heisenberg equations of motion are

$$\frac{d}{dt}\hat{K}_x = -\frac{1}{\hbar}[\nu_0 + \nu_m\sin(\omega t)]\,\hat{K}_y, \tag{15}$$

$$\frac{d}{dt}\hat{K}_y = \frac{1}{\hbar}[\nu_0 + \nu_m\sin(\omega t)]\,\hat{K}_x - \frac{\eta}{\hbar}\frac{\sqrt{2}}{N} + \frac{\eta}{\hbar}\frac{3\sqrt{2}}{4}\left(\hat{K}_z - 1\right)\left(\hat{K}_z + \frac{1}{3}\right), \tag{16}$$

$$\frac{d}{dt}\hat{K}_z = \frac{\eta}{\hbar}\sqrt{2}\hat{K}_y. \tag{17}$$

For a strongly condensed case and large particle number, it is appropriate to take K_x, K_y, and K_z as three real numbers u, v, and w, respectively. Then we get the mean-field Heisenberg equations

$$\frac{d}{dt}u = -\frac{1}{\hbar}[\nu_0 + \nu_m\sin(\omega t)]\,v, \tag{18}$$

$$\frac{d}{dt}v = \frac{1}{\hbar}[\nu_0 + \nu_m\sin(\omega t)]\,u + \frac{\eta}{\hbar}\frac{3\sqrt{2}}{4}(w - 1)\left(w + \frac{1}{3}\right), \tag{19}$$

$$\frac{d}{dt}w = \frac{\eta}{\hbar}\sqrt{2}v. \tag{20}$$

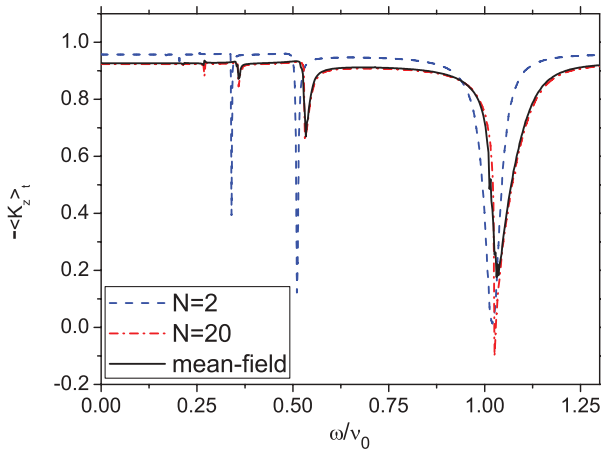

FIG. 1. (Color online) Time-averaged population imbalance $-\langle \hat{K}_z \rangle_t$ for the driven system with different numbers of particles, tilt $\nu_0/\eta = 5$, and scaled driving amplitude $\nu_m = 1$.

To get the time-averaged value of the conversion varied with different external fields, we characterize each quantum trajectory by its time-averaged imbalance

$$-\langle \hat{K}_z \rangle_t \equiv -\frac{1}{\Delta t}\int_0^{\Delta t} dt \langle \hat{K}_z \rangle(t), \tag{21}$$

employing the averaging interval $\Delta t \gg \hbar/\nu_0$. Initially, all particles are atoms. Figure 1 shows the results of such calculations by numerically solving the Heisenberg equations (15)–(17) for $N = 2$ and 20 under periodic modulation with the fixed scaled amplitude $\nu_m/\nu_0 = 0.2$ and frequencies ω ranging from 0 to $1.25\nu_0$. The solution of the mean-field equations (18)–(20) is also presented. There are several clear spikes that indicate the Shapiro-like resonance in atom-molecule conversion driven by the external magnetic field.

These spikes indicate that the frequency of the modulated field is commensurate with the intrinsic frequencies of the atom-molecule conversion system in the absence of the periodic modulation. Now we analyze the intrinsic frequency. For $N = 2$, using the Fock state as the basis, the commutators (11)–(13) becomes

$$[\hat{K}_z, \hat{K}_x] = 2i\hat{K}_y, \quad [\hat{K}_z, \hat{L}_y] = -2i\hat{K}_x, \tag{22}$$

$$[\hat{K}_x, \hat{K}_y] = i\hat{K}_z. \tag{23}$$

From the Heisenberg equations (15)–(17), we get

$$\frac{d^2}{dt^2}\hat{K}_y + \frac{1}{\hbar^2}\left(\nu_0^2 + \eta^2\right)\hat{K}_y = 0. \tag{24}$$

Then the intrinsic frequency is readily obtained from the above equation as $\sqrt{\nu_0^2 + \eta^2}/\hbar$. Thus, the center of resonance is expected to be $\sqrt{\nu_0^2 + \eta^2}/(\hbar\omega) = p/q$ with p and q as integers. In our case, the resonances corresponding to $p/q = 1, 2, 3$ are more prominent. With N increasing, we find that the resonance center shifts to the right due to the many-body effect. We can obtain the intrinsic frequency in the mean-field limit, i.e., $N \to \infty$. From the mean-field equations (18)–(20), we readily obtain

$$\frac{d^2}{dt^2}v + \frac{1}{\hbar^2}\left[\nu_0^2 + \eta^2(1 - 3w)\right]v = 0. \tag{25}$$

Initially all particles are in atom states, i.e., $w = -1$. Approximately substituting it into the above equation, we obtain the explicit expression of the frequency $\sqrt{\nu_0^2 + 4\eta^2}/\hbar$. This implies that, due to the many-body effect [23], the resonance center shifts to $\sqrt{\nu_0^2 + 4\eta^2}/(\hbar\omega) = 1, 2, 3, \ldots$. The above theoretical analysis agrees with our numerical results.

C. Phase space at the Shapiro-like resonance

The Shapiro resonance phenomenon can be demonstrated intuitively by the trajectories in the phase space of the system. Notice that the constraint $u^2 + v^2 = \frac{1}{2}(w-1)^2(w+1)$, and introducing the canonical variable $s = w$, and $\theta = \arctan(v/u)$ denoting the population imbalance and the relative phase between atoms and molecules, the mean-field Heisenberg equations can be replaced by a classical Hamiltonian of the form

$$\mathcal{H} = \frac{1}{\hbar}\left[\nu_0 + \nu_m \sin(\omega t)\right]s + \frac{\eta}{\hbar}\sqrt{(s-1)^2(s+1)}\cos\theta, \tag{26}$$

and the canonical equations of motion are

$$\frac{d\theta}{dt} = \frac{\partial \mathcal{H}}{\partial s} = \frac{1}{\hbar}\left[\nu_0 + \nu_m \sin(\omega t)\right] - \frac{\eta}{\hbar}\frac{(1+3s)}{2\sqrt{1+s}}\cos\theta, \tag{27}$$

$$\frac{ds}{dt} = -\frac{\partial \mathcal{H}}{\partial \theta} = \frac{\eta}{\hbar}\sqrt{(1-s)^2(1+s)}\sin\theta. \tag{28}$$

Using a generation function

$$F(\theta, S) = \left[\theta - \frac{\nu_0 t}{\hbar} + \frac{\nu_m}{\hbar\omega}\cos(\omega t)\right]S, \tag{29}$$

with the following relations

$$s = \frac{\partial F}{\partial \theta} = S, \tag{30}$$

$$\Theta = \frac{\partial F}{\partial S} = \left[\theta - \frac{\nu_0 t}{\hbar} + \frac{\nu_m}{\hbar\omega}\cos(\omega t)\right], \tag{31}$$

we obtain the new Hamiltonian

$$\begin{aligned}\mathcal{K}(S, \Theta) &= \mathcal{H} + \frac{\partial F}{\partial t} \\ &= \frac{\eta}{\hbar}\sqrt{(1-S)^2(1+S)} \\ &\quad \cos\left[\Theta + \frac{\nu_0 t}{\hbar} - \frac{\nu_m}{\hbar\omega}\cos(\omega t)\right].\end{aligned} \tag{32}$$

The secular evolution of S and Θ can be evaluated from the time-averaged Hamiltonian

$$\langle \mathcal{K}(S, \Theta)\rangle_T = \frac{1}{T}\int_0^T \mathcal{K}(S, \Theta)\, dt, \tag{33}$$

with $T = 2\pi/\omega$.

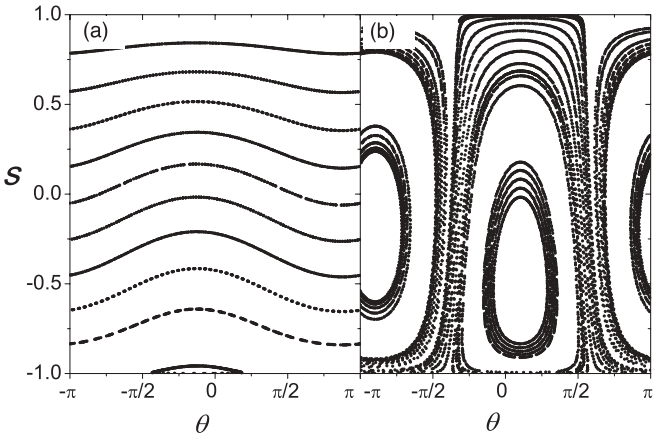

FIG. 2. Poincaré section of the classical Hamiltonian (26) with tilt $\nu_0/\eta = 24$, scaled driving amplitude $\nu_m = 0.2\nu_0$, and modulation frequency (a) $\omega/\nu_0 = 0.95$ (off resonance) and (b) $\omega/\nu_0 = 1$ (near resonance).

Now, we consider the 1:1 resonance case that $\hbar\omega \approx \nu_0$,

$$\langle \mathcal{K}(S,\Theta)\rangle_T \approx J_1\left(\frac{\nu_m}{\nu_0}\right)\frac{\eta}{\hbar}\sqrt{(1-S)^2(1+S)}\sin\Theta. \quad (34)$$

where $J_1(x)$ is the first-kind Bessel function. The phase graph of the periodic averaged Hamiltonian system reflects the Poincaré section of the Hamiltonian system (26), as shown in Fig. 2. For the case of off-resonance, the integral in Eq. (33) approximates to zero, which implies that the time-averaged s varies a little in time, while the variable θ increases with time almost linearly. The corresponding Poincaré section is shown in Fig. 2(b). It is shown that the phase space at the transition changes dramatically.

D. Intrinsic resonance width: Arnold tongues

For the initial condition $s = w = 1$, whether its trajectory falls into a resonance regime can be judged from the following resonance condition: $\Delta\mathcal{H} > 2\nu_0/\hbar$, where $\Delta\mathcal{H}$ is the difference between the maximum and the minimum value of $\mathcal{H}$ in the time interval $\Delta t \gg \hbar/\nu_0$. For different ν_m and ω, we obtain the regions in the two-dimensional parameter space where the resonance emerges. These regions are named Arnold tongues [24]. To draw out the Arnold tongues in parameter space, the main numerical tool used in this work is the winding number $\mathcal{W}$

$$\mathcal{W} = \lim_{t\to\infty}\frac{\theta(t)-\theta(0)}{t}, \quad (35)$$

with initial conditions $[\theta(0), s(0)]$. If the ratio $\mathcal{W}/\omega$ is rational, i.e., $\mathcal{W}/\omega = q/p$, here q and p are natural numbers, then $[\theta(t), s(t)]$ is a resonant solution of $(q:p)$ type, i.e.,

$$[\theta(t+pT), s(t+pT)] = [\theta(t), s(t)] + (2\pi q, 0), \quad (36)$$

which means the system runs q times in the time pT interval. In our system, only $(q:1)$ type is significant. In Fig. 3, we show the first five resonance regions with $\nu_0/\eta = 5$. The width of the resonance regions is broadened as the modulation amplitude ν_m increases.

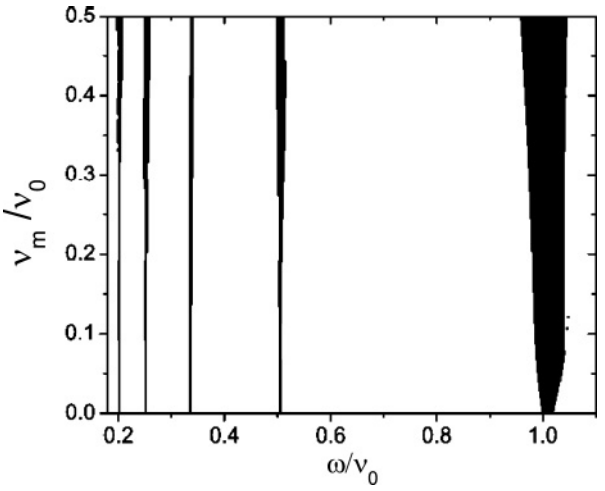

FIG. 3. Arnold tongues for resonance modes (1:1), (2:1), (3:1), (4:1), and (5:1), from right to left, with $\nu_0/\eta = 5$.

III. APPLICATION TO EXPERIMENT

A. Noncondensed atoms

The generation of cold dimers from a cold Bose gas using an oscillating magnetic field, rather than the more often studied linear sweep through a Feshbach resonance, has been implemented experimentally by the Wieman group at JILA [19]. Their study showed that the method works and provides substantial data. The advantage of this method is that it greatly reduces the heating the cloud experiences in the conversion process, because the conversion mainly occurs far from the center of the Feshbach resonance. In a practical experiment in which the atoms are not condensed, the many modes are strongly coupled, and the full Hamiltonian will read

$$\hat{H}^c = \sum_p(\epsilon_{a,p}-\mu)\hat{a}_p^\dagger\hat{a}_p + \sum_q[\epsilon_{b,q}+\nu(t)-2\mu]\hat{b}_q^\dagger\hat{b}_q + \frac{g}{\sqrt{\mathcal{V}}}\sum_{p,q}(\hat{a}_{p+q/2}^\dagger\hat{a}_{-p+q/2}^\dagger\hat{b}_q + \hat{b}_q^\dagger\hat{a}_{-p+q/2}\hat{a}_{p+q/2}). \quad (37)$$

The kinetic-energy distribution of the thermal particles are characterized by k_BT, here k_B is the Boltzman constant, and T is the temperature. In the experiment, k_BT is much smaller than the effective Feshbach resonance width $g\sqrt{n}$, therefore we ignore the variation in the kinetic energy, i.e., $\epsilon_{a,p} \to \epsilon_a$ and $\epsilon_{b,q} \to \epsilon_b$. This approximation is tantamount to denoting each "energy band" of the thermal particles by one energy level, as schematically plotted by Fig. 4. In such an approximation, the Hamiltonian (37) reduces to Eq. (1).

The above single-mode approximation has been successfully applied to explain the data of Feshbach atom-molecule conversion with a linear sweep [23]. For a long time evolution, thermal particles scattering off the single-mode mean field will cause phase diffusion at a rate proportional to the thermal cloud temperature, i.e., $\gamma = 1/\tau_d = k_BT/(2\pi\hbar)$. Here, $\tau_d = 2\pi\hbar/(k_BT)$ is the dephasing time [25]. To account for the experimental data, we need to include the dephasing effect in our model. Modeling dephasing by fully including the quantum effects requires sophisticated theoretical studies. The

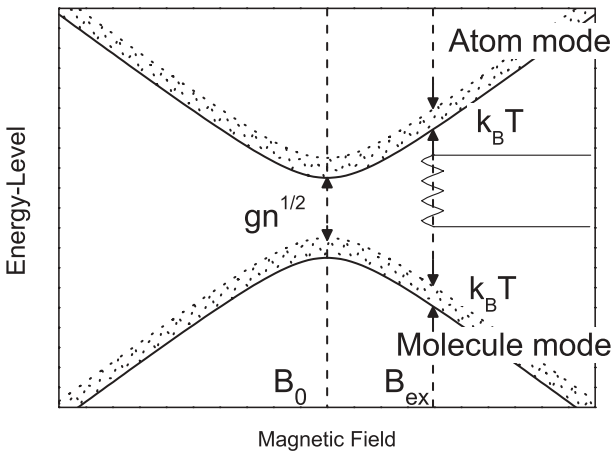

FIG. 4. Schematic of the swept magnetic field in the experiment. See text for details.

standard approaches of quantum optics for open systems involve quantum kinetic master equations. Here, we adopt the simple mean-field treatment in our model. From the mean-field viewpoint, the decoherence term introduces a γ transversal relaxation term into the mean-field equations of motion according to [26,27],

$$\frac{d}{dt}u = -\frac{1}{\hbar}[\nu(t) + \epsilon_b - 2\epsilon_a]v - \gamma u, \tag{38}$$

$$\frac{d}{dt}v = \frac{1}{\hbar}[\nu(t) + \epsilon_b - 2\epsilon_a]u + \frac{\eta}{\hbar}\frac{3}{4}\sqrt{2}(w-1)\left(w + \frac{1}{3}\right) - \gamma v, \tag{39}$$

$$\frac{d}{dt}w = \frac{\eta}{\hbar}\sqrt{2}v. \tag{40}$$

The imbalance of atom pairs and molecules w is varied in the range of $[-1, 1]$ with the lower limit corresponding to a pure atomic gas and $w = 1$ for a pure molecular gas. What we are concerned about is, after the conversion process, how many atomic pairs are converted to molecules. We use w_f to denote the value of w when the magnetic field sweeps back. The molecular conversion efficiency can be read from the variable w_f as $\Gamma = (1 + w_f)/2$.

Now we apply our theory to the experiment of ^{85}Rb by Ref. [19]. The atoms are held in a purely magnetic trap at a bias field of B_r. After evaporative cooling, the magnetic field B is linearly swept to a selected value at $B_{\rm ex}$, and then a sinusoidal magnetic-field pulse with peak-to-peak amplitude $B_{\rm mod}$ and modulation frequency ω for a duration of the coupling time is applied. The swept magnetic field can be expressed as

$$B = \begin{cases} B_r - \alpha t & 0 \leqslant t < t_0, \\ B_{\rm ex} + B_{\rm mod}\sin(\omega t) & t_0 \leqslant t < t_0 + t_c, \\ B_{\rm ex} + \alpha t & t_0 + t_c \leqslant t < 2t_0 + t_c. \end{cases} \tag{41}$$

Here, $B_r = 162$ G, $B_{\rm ex} = 156.5$ G, $B_{\rm mod} = 0.13$ G, ω ranges from 2 to 9 kHz, t_0 is the linear sweep time, $\alpha = (B_r - B_{\rm ex})/t_0$ is the linear sweep rate, and t_c is the coupling time. The sketch curve is shown in Fig. 4. For the thermal cloud, with temperature T, one molecule has *five* degrees of freedom while two atoms have six degrees of freedom; according to the equipartition theorem, we have $(2\epsilon_a - \epsilon_b) \approx k_B T/2$. The scaled parameters in Eqs. (38)–(40) are

$$\nu(t) = -\frac{\hbar^2}{m a_{\rm bg}^2}\frac{(B - B_0)^2}{\left[\left(1 - \frac{r_0}{a_{\rm bg}}\right)(B - B_0) - \Delta B\right]^2}, \tag{42}$$

and

$$\eta = 2\sqrt{4\pi\hbar^2 |a_{\rm bg}\Delta\mu|\Delta B n/m}. \tag{43}$$

The experimental parameters are $a_{\rm bg} = -443a_0$, $r_0 = 185a_0$ [28], $\Delta B = 10.71$ G, $B_0 = 155$ G, $\Delta\mu = 1.2 \times 10^{-4}\mu_B$, temperature $T = 20$ nK, and density $n = 10^{11}$ cm^{-3}; here a_0 and μ_B are the Bohr radius and Bohr magneton, respectively. The difference of magnetic moment $\Delta\mu$ is extracted from the experimental data [29]. Under this condition, the ratio between the kinetic-energy distribution of thermal particles and the effective Feshbach resonance width, i.e., $k_B T/(g\sqrt{n})$, is estimated to be 0.05, much smaller than unity. Figure 5 shows the conversion efficiency as a function of modulation frequency for three different coupling times. The resonance linewidth is broadened by the dephasing term. There is a clear Lorentzian distribution resonance at a frequency of about 6.25 kHz, close to the experiment. Besides the fundamental frequency resonance at $\omega = 6.25$ kHz, there is also a weak (2:1) mode resonance at about $\omega = 3.1$ kHz, which has not been observed in an experiment. Our linewidth is approximately 0.3 kHz at the zero conversion limit, as shown in the inset in Fig. 5. In the experiment, it is about 0.2 kHz.

In Ref. [20], the conversion efficiency is given by a weighted average of the two-body transition probability density ρ over a Maxwell distribution. For the long coupling time limit, i.e., $t_f \to \infty$ in Ref. [20], the two-body transition probability density ρ can be approximated by $\rho \propto \delta(E_b^{\rm av} + \hbar\omega_{\rm mod} - p_{\rm res}^2/m)$. Then one could get $\Gamma = 2N_{\rm mol}/N \propto \sqrt{E_b^{\rm av} + \hbar\omega_{\rm mod}}\exp[-\beta(E_b^{\rm av} + \hbar\omega_{\rm mod})]$. This is an

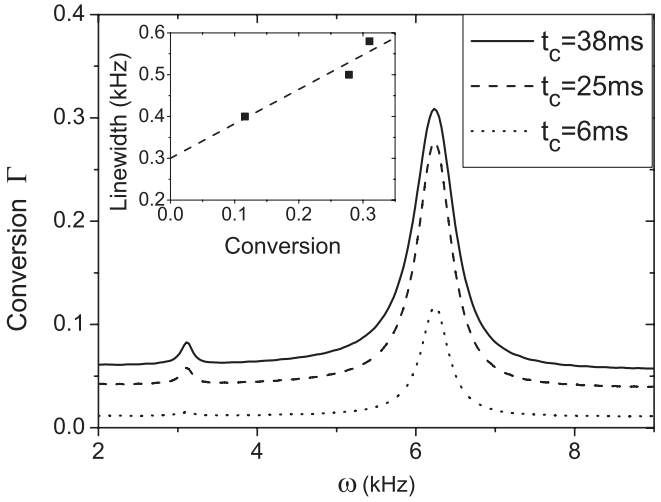

FIG. 5. Conversion efficiency of atoms converted to molecules as a function of modulation frequency for three different coupling times. For a fixed coupling time, the curve can be fitted by a Lorentzian distribution $\Gamma = \Gamma_0 + \frac{2A}{\pi}\frac{\Delta}{4(\omega-\omega_c)^2+\Delta^2}$; e.g., for $t_c = 38$ ms, the fitting parameters are $\Gamma_0 = 0.06$, $\omega_c = 6.2$, $\Delta = 0.6$, and $A = 0.23$. In the inset, by fitting the linewidth vs conversion data to a straight line, we find the zero conversion limit to be 0.3 kHz.

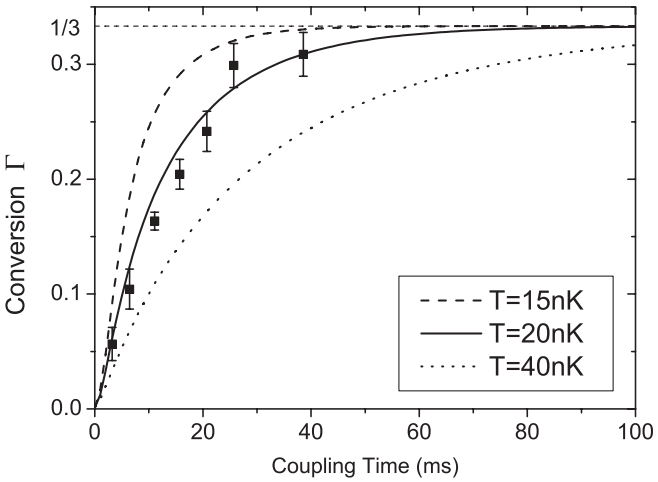

FIG. 6. Conversion efficiency of atoms converted to molecules under a periodic modulation with amplitude $B_{\rm mod} = 0.13$ G and frequency $\omega = 6.25$ kHz with respect to coupling time for different temperatures. The squares with error bars are from Fig. 4(a) of Ref. [19]. The conversion of ultracold atoms to molecules increases with the coupling time until it becomes saturated at 1/3.

asymmetric Γ distribution, departing from the observed Lorentzian-like resonance profiles.

In our calculation, we find that in the three stages of magnetic-field change expressed by Eq. (41), the linear process contributes little to the atom-molecule conversion. This is because the oscillation center $B_{\rm ex}$ is still far away from the Feshbach resonance center. The atom-molecule conversion mainly occurs in the process of applying the sinusoidal magnetic field, where $\nu(t)$ can be expressed as $\nu_0 + \nu_m \sin(\omega t)$. Therefore, the above observed resonance phenomenon corresponds to the Shapiro resonance discussed in Sec. II, while the linewidth is dramatically broadened by the thermal dephasing effect.

In Fig. 6, we show the conversion efficiency with respect to coupling time. The squares with error bars are experimental data in Ref. [19]. For temperature $T = 20$ nK and density $n = 10^{11}$ cm^{-3}, our results are close to the experimental data. We also show the cases of different temperatures by considering the isobaric condition, i.e., $nT = $ const. The above calculation shows that increasing the temperature will lessen the molecular production because the dephasing term is proportional to the temperature. On the other aspect, the conversion efficiency decreases with the increasing temperature. For different temperatures, a common feature is that the conversion efficiency increases with the coupling time until the conversion efficiency becomes saturated at 1/3. This can be explained by investigating Eqs. (38)–(40), where $u = v = 0$ and $w = -1/3$ is the fixed point in the absence of the dephasing term. The observed limit in the atom-molecule conversion efficiency has been extensively discussed, including the Landau-Zener (LZ) model of two-body molecular production [30], phase-space density model [31], equilibration model at finite temperatures [32], and nonlinear particle interaction model [33]. Our present investigation suggests a new mechanism for the observed maximum efficiency: the system is found to relax into the mean-field fixed point due to the dephasing effect.

Finally, we would like to discuss our single-mode approximation. This approximation is expected to work well only for the strongly condensed case. The validity of the above two-mode classical model in the noncondensed case is not clear. For the noncondensed case, the Bose gas usually needs a more delicate treatment, because the particles are distributed over many spatial modes. However, since bosonic occupation numbers can become large at low temperatures even above the BEC transition temperature, our above calculations suggest that the two-mode classical model might be applicable in this case. This idea is consistent with recent work by Castin, Gardiner, and others [34].

B. Condensed atoms

In this section, we extend our discussion to the case of condensed atoms. The main source of dephasing in a BEC is the thermal cloud of particles surrounding the condensate. Thermal particles scattering off the condensate will produce a dephasing rate γ proportional to the thermal cloud temperature. The dephasing rate will go down as the thermal fraction decreases and become negligible at extremely low temperature. The dephasing rate can be estimated as $\gamma = 8\pi^3(8\pi a_{\rm eff}^2 n_{\rm th}\overline{v})$ [35]. The bracketed term is the elastic collision rate due to noncondensed atoms in the thermal cloud. It is the product of the scattering cross section for identical particles (8π times the square of the s-wave scattering length $a_{\rm eff}$), the number density of noncondensed atoms $n_{\rm th}$, and their thermal velocity at temperature T, $\overline{v} = \sqrt{2k_BT/m}$. Using the parameters of ^{85}Rb, $n_{\rm th} = 10^{10}$ m^{-3} [35], we have $\gamma \simeq 10^{-3}$ Hz at $T = 100$ nK. It is negligible for our following calculations. Actually, for a pure BEC, the interaction between the coherent atoms becomes important. After ignoring the kinetic energies of particles, the Hamiltonian can be written as

$$\hat{H} = \nu(t)\hat{b}^\dagger\hat{b} - \frac{U}{\mathcal{V}}\hat{a}^\dagger\hat{a}^\dagger\hat{a}\hat{a} + \frac{g}{\sqrt{\mathcal{V}}}(\hat{a}^\dagger\hat{a}^\dagger\hat{b} + \hat{b}^\dagger\hat{a}\hat{a}),$$

where $U = 4\pi\hbar^2|a_{\rm bg}|/m$ denotes the nonlinear interaction. In the mean-field limit, we can derive the Heisenberg equations of motion as

$$\frac{d}{dt}u = -\frac{\nu(t)}{\hbar}v - \frac{2Un}{\hbar}v(1-w), \tag{44}$$

$$\frac{d}{dt}v = \frac{\nu(t)}{\hbar}u + \frac{\eta}{\hbar}\frac{3}{4}\sqrt{2}(w-1)\left(w+\frac{1}{3}\right) + \frac{2Un}{\hbar}u(1-w), \tag{45}$$

$$\frac{d}{dt}w = \frac{\eta}{\hbar}\sqrt{2}v. \tag{46}$$

Figure 7 presents the conversion efficiency under a periodic modulation with fixed amplitude $B_{\rm mod} = 0.5$ G and different frequencies by numerically solving Eqs. (44)–(46). The density for the condensed atoms is $n = 10^{12}$ cm^{-3}, and thereby the scaled nonlinear interaction is $Un/\eta = 0.14$. One sees that there is a Rabi oscillation that can reach a high conversion efficiency. In the experiment, they observe 55% conversion for coupling time 1.6 ms [19]. The observation marked by a dark triangle in Fig. 7 is consistent with our result.

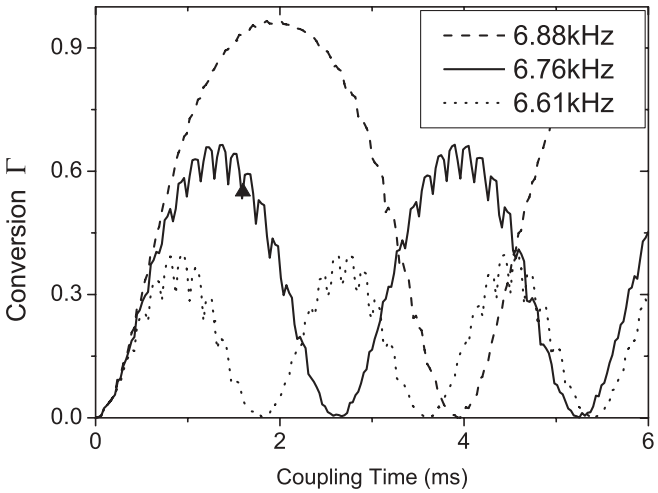

FIG. 7. The conversion efficiency from condensed atoms to molecules under a periodic modulation with fixed amplitude $B_{\mathrm{mod}} = 0.5$ G and different frequencies. The density for the condensed atoms is $n = 10^{12}$ cm^{-3}. The dark triangle marks the experimental observation in Ref. [19].

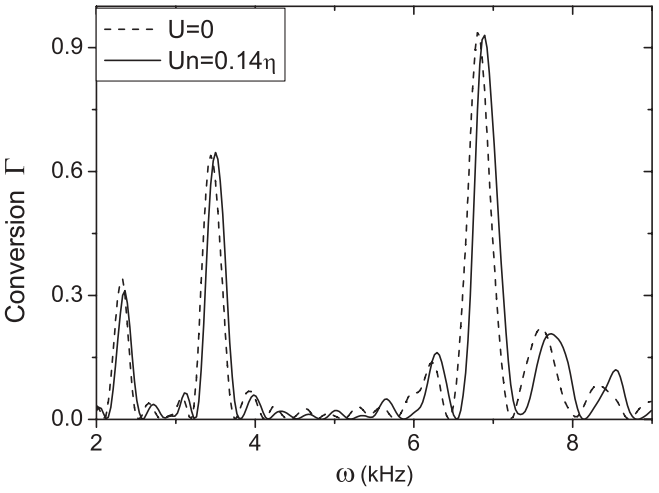

FIG. 8. The conversion efficiency from condensed atoms to molecules with respect to modulation frequency for different nonlinear interactions U. The coupling time is 1.6 ms. The other parameters are the same as in Fig. 7.

Figure 8 presents the conversion efficiency with respect to modulation frequency for different nonlinear interactions U. The coupling time for this calculation is 1.6 ms. The other parameters are the same as in Fig. 7. In Fig. 8, we observe some oscillations besides the main resonance peaks and find that the maximum conversion efficiency could be far beyond the limit 1/3. Because the resonance center can be still approximated by $\omega = \sqrt{\nu_e^2 + 4\eta^2}/\hbar$, it implicitly depends on the density through parameter η. In the experiment, the density of the condensed atoms is about ten times larger than that of the thermal cloud; therefore, the resonance center shifts to the right-hand side when compared to the thermal atomic cloud case in Fig. 5. Moreover, we find that the interaction between the coherent atoms will lead to the shift of the resonance profile, as clearly shown in Fig. 8.

IV. CONCLUSIONS

In conclusion, we have thoroughly investigated the mechanism underlying the Shapiro resonance phenomenon in the atom-molecule conversion by exploiting a microscopic two-channel model. With the inclusion of the thermal dephasing effect in the noncondensed atom clouds, our model could account for most experimental observations. We also extend our discussions to the case of condensed atoms. Our theory has some interesting predictions waiting for future experimental testing.

ACKNOWLEDGMENTS

This work is supported by the National Natural Science Foundation of China (Nos. 10725521, 10604009), and the 973 project of China under Grant Nos. 2006CB921400 and 2007CB814800.

[1] S. Shapiro, Phys. Rev. Lett. **11**, 80 (1963).
[2] A. Barone and G. Paternò, *Physics and Applications of the Josephson Effect* (Wiley, New York, 1982).
[3] F. Bloch, Phys. Rev. B **2**, 109 (1970).
[4] T. A. Fulton, Phys. Rev. B **7**, 981 (1973).
[5] B. N. Taylor, W. H. Parker, D. N. Langenberg, and A. Denestein, Metrologia **3**, 89 (1967).
[6] R. Pöpel, Metrologia **29**, 153 (1992).
[7] S. Raghavan, A. Smerzi, S. Fantoni, and S. R. Shenoy, Phys. Rev. A **59**, 620 (1999).
[8] André Eckardt, Tharanga Jinasundera, Christoph Weiss, and Martin Holthaus, Phys. Rev. Lett. **95**, 200401 (2005).
[9] Sigmund Kohler and Fernando Sols, New J. Phys. **5**, 94 (2003).
[10] M. Greiner, C. A. Regal, and D. S. Jin, Nature (London) **426**, 537 (2003).
[11] M. W. Zwierlein, C. A. Stan, C. H. Schunck, S. M. F. Raupach, S. Gupta, Z. Hadzibabic, and W. Ketterle, Phys. Rev. Lett. **91**, 250401 (2003).
[12] S. Jochim, M. Bartenstein, A. Altmeyer, G. Hendl, S. Riedl, C. Chin, J. Hecker Denschlag, and R. Grimm, Science **302**, 2101 (2003).
[13] M. Bartenstein, A. Altmeyer, S. Riedl, S. Jochim, C. Chin, J. H. Denschlag, and R. Grimm, Phys. Rev. Lett. **92**, 120401 (2004).
[14] E. A. Donley, N. R. Claussen, S. T. Thompson, and C. E. Wieman, Nature (London) **417**, 529 (2002).
[15] M. Holland, S. J. J. M. F. Kokkelmans, M. L. Chiofalo, and R. Walser, Phys. Rev. Lett. **87**, 120406 (2001).
[16] E. Timmermans, K. Furuya, P. W. Milloni, and A. K. Kerman, Phys. Lett. **A285**, 228 (2001).
[17] M. W. Zwierlein, C. A. Stan, C. H. Schunck, S. M. F. Raupach, A. J. Kerman, and W. Ketterle, Phys. Rev. Lett. **92**, 120403 (2004).
[18] M. Greiner, C. A. Regal, and D. S. Jin, Phys. Rev. Lett. **94**, 070403 (2005).
[19] S. T. Thompson, E. Hodby, and C. E. Wieman, Phys. Rev. Lett. **95**, 190404 (2005).

[20] Thomas M. Hanna, Thorsten Köhler, and Keith Burnett, Phys. Rev. A **75**, 013606 (2007).
[21] Thorsten Köhler and Krzysztof Góral, Rev. Mod. Phys. **78**, 1311 (2006).
[22] A. Vardi, V. A. Yurovsky, and J. R. Anglin, Phys. Rev. A **64**, 063611 (2001).
[23] Jie Liu, Bin Liu, and Li-Bin Fu, Phys. Rev. A **78**, 013618 (2008).
[24] V. I. Arnold, Trans. Am. Math. Soc., Ser. 2 **46**, 213 (1965).
[25] See, for example, E. Eisenberg, K. Held, and B. L. Altshuler, Phys. Rev. Lett. **88**, 136801 (2002).
[26] Jie Liu, Chuan-wei Zhang, Mark G. Raizen, and Qian Niu, Phys. Rev. A **73**, 013601 (2006).
[27] J. R. Anglin and A. Vardi, Phys. Rev. A **64**, 013605 (2001).
[28] R. A. Duine and H. T. C. Stoof, New J. Phys. **5**, 69 (2003); G. F. Gribakin and V. V. Flambaum, Phys. Rev. A **48**, 546 (1993).
[29] N. R. Claussen, S. J. J. M. F. Kokkelmans, S. T. Thompson, E. A. Donley, E. Hodby, and C. E. Wieman, Phys. Rev. A **67**, 060701(R) (2003).
[30] Krzysztof Goral, Thorsten Koehler, Simon A. Gardiner, Eite Tiesinga, and Paul S. Julienne, J. Phys. B **37**, 3457 (2004).
[31] E. Hodby, S. T. Thompson, C. A. Regal, M. Greiner, A. C. Wilson, D. S. Jin, E. A. Cornell, and C. E. Wieman, Phys. Rev. Lett. **94**, 120402 (2005).
[32] J. E. Williams, N. Nygaard, and C. W. Clark, New J. Phys. **8**, 150 (2006).
[33] Jie Liu, Li-Bin Fu, Bin Liu, and Biao Wu, New J. Phys. **10**, 123018 (2008).
[34] A. Sinatra and Y. Castin, Phys. Rev. A **78**, 053615 (2008); A. Sinatra, Y. Castin, and E. Witkowska, *ibid.* **80**, 033614 (2009); A. A. Norrie, R. J. Ballagh, and C. W. Gardiner, *ibid.* **73**, 043617 (2006).
[35] Diego A. R. Dalvit, Jacek Dziarmaga, and Wojciech H. Zurek, Phys. Rev. A **62**, 013607 (2000); P. J. Y. Louis, P. M. R. Brydon, and C. M. Savage, *ibid.* **64**, 053613 (2001).